AAPT PHYSICS EDUCATION | AMERICAN JOURNAL of PHYSICS

Quantum solutions for a symmetric double square well

Edward A. Johnson and H. Thomas Williams

Citation: American Journal of Physics **50**, 239 (1982); doi: 10.1119/1.13046
View online: http://dx.doi.org/10.1119/1.13046
View Table of Contents: http://scitation.aip.org/content/aapt/journal/ajp/50/3?ver=pdfcov
Published by the American Association of Physics Teachers

Quantum solutions for a symmetric double square well

Edward A. Johnson and H. Thomas Williams
Department of Physics, Washington and Lee University, Lexington, Virginia 24450

(Received 23 February 1981; accepted for publication 20 May 1981)

The quantum behavior of a wave packet in a one-dimensional infinite square well with a finite barrier in the center is considered. Computer generated plots are presented that lead to useful analytic approximations for finding eigenvalues of the Schrödinger equation and for explaining the time dependence of wave packets.

I. INTRODUCTION

The project that generated this work began as an attempt to produce a one-dimensional, nonrelativistic model for off-mass-shell scattering. Using graphics techniques like those of Goldberg, Schey, and Schwartz,[1] a systematic study of the scattering of bound-state wave functions, as exemplified in Segre and Sullivan,[2] was proposed. At present, we are short of our goal, yet the use of computer graphics has already produced insights into the behavior of certain bound-state wave packets, which have led to useful "semi-analytical" results. We describe two such results, relating to the determination of energy levels of an infinite well with a finite central barrier, and the "regeneration period" of a wave packet in a potential well.

This work began as an assignment in an undergraduate, one-semester quantum mechanics course, and grew into a senior thesis topic. The physical ideas involved are within the grasp of undergraduate physics majors, and needed computer experience, equipment, and mathematical techniques are also not unusual within undergraduate programs. The problem is presented as an example of a large class of straightforward quantum mechanics projects within the capabilities of good undergraduate physics majors, and with clear analogies to interesting physical systems.

II. PROBLEM

We propose to study the time evolution of a wave packet bound in a well containing a barrier. The simplest such quantum-mechanical system is that of a wave packet bound in a symmetric double well—a rectangular potential barrier centered in an infinite square well (Fig. 1). The wave packet is constructed of a linear combination of solutions (eigenfunctions) of the time-dependent Schrödinger equation corresponding to specific energy levels (eigenvalues). Individual wave functions are found by solving the time-dependent Schrödinger equation:

$$\frac{-\hbar^2}{2m}\frac{\partial^2}{\partial x^2}\Psi(x,t)+V\Psi(x,t)=-i\hbar\frac{\partial}{\partial t}\Psi(x,t). \tag{1}$$

Solving this for the spectrum of eigenvalues and corresponding eigenfunctions, linear combinations with desired properties can be formed, and their development in time can be studied.

III. SOLUTION

Eigenvalues and eigenfunctions for piecewise continuous potentials such as those of Fig. 1 are straightforwardly found, using techniques familiar from most introductory texts (see, for example, Ref. 3—the "hands on" approach of this book is much in the spirit of the present work). Formally, the eigenfunctions of this potential are (using the notation of Fig. 1):

$$\Psi(x,t)=A\sin\left(\frac{(2mE)^{1/2}}{\hbar}x\right)\exp\left(\frac{-iE}{\hbar}t\right); \tag{2}$$

in region II, for energies below the barrier height,

$$\Psi(x,t)=\left[B\exp\left(\frac{[2m(V_2-E)]^{1/2}}{\hbar}x\right)+C\exp\left(\frac{-[2m(V_2-E)]^{1/2}}{\hbar}x\right)\right]\exp\left(\frac{-iE}{\hbar}t\right); \tag{3}$$

in region II, for energies above the barrier height,

$$\Psi(x,t)=\left[B\sin\left(\frac{[2m(V_2-E)]^{1/2}}{\hbar}x\right)+C\cos\left(\frac{[2m(V_2-E)]^{1/2}}{\hbar}x\right)\right]\exp\left(\frac{-iE}{\hbar}t\right); \tag{4}$$

and in region III,

$$\Psi(x,t)=D\sin\left(\frac{(2mE)^{1/2}}{\hbar}(x-L_3)\right)\exp\left(\frac{-iE}{\hbar}t\right). \tag{5}$$

The coefficients A, B, C, and D, as well as the energy eigenvalues E, are determined (to within the overall normalization of the wave function) by enforcing continuity of $\Psi(x,t)$ and its spatial derivative at the discontinuities in the potential at $x=L_1$ and $x=L_2$. These conditions yield equations for three of the four coefficients:

$$B/A=\tfrac{1}{2}\exp(-k_2L_1)\times[\sin(k_1L_1)+(k_1/k_2)\cos(k_1L_1)], \tag{6}$$

$$C/A=\tfrac{1}{2}\exp(k_2L_1)\times[\sin(k_1L_1)-(k_1/k_2)\cos(k_1L_1)], \tag{7}$$

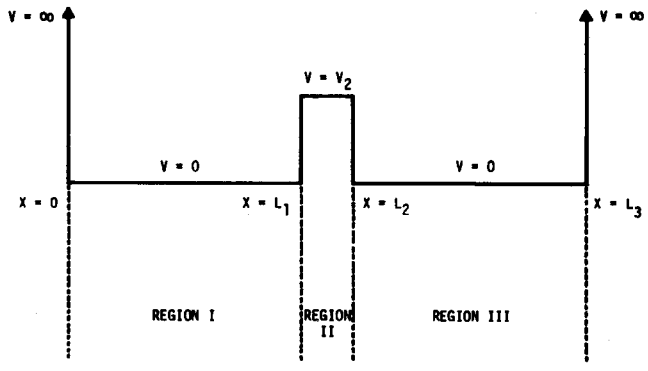

Fig. 1. Symmetric double well along with the notation used in the paper.

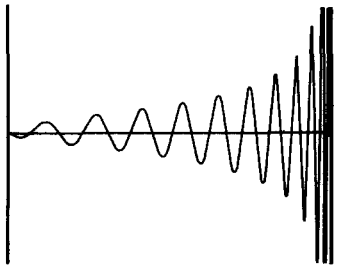

Fig. 2. Energy level function for a near-zero barrier is similar to that of an infinite square well.

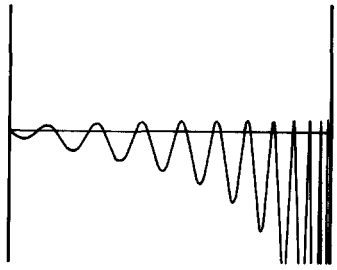

Fig. 4. Function for a 0.5% barrier.

and

$$D/A = -\cosh[k_2(L_2 - L_1)] - (k_1/k_2)\cot(k_1L_1)\sinh[k_2(L_2 - L_1)], \quad (8)$$

where $k_1 = (2ME)^{1/2}/\hbar$ and $k_2 = [2M(V_2 - E)]^{1/2}/\hbar$. A transcendental equation whose solutions are the energy eigenvalues E, is also found:

$$\tanh[k_2(L_2 - L_1)][(k_2/k_1)^2\sin^2(k_1L_1) + \cos^2(k_1L_1)] + 2(k_2/k_1)\sin(k_1L_1)\cos(k_1L_1) = 0. \quad (9)$$

To be sure, this equation is only indifferently tractable and in difficult cases, a numerical solution requires patience and a great deal of computer time. Instead of this equation, our final calculations use a semianalytical interpolation scheme (discussed later in this section) that exploits the double well's inherent symmetry. However, we present this formal solution as well since a study of Eq. (9) through computer plots and numerical solutions reveals several interesting facts.

In Figs. 2–5, the total energy E is plotted along the horizontal axis from $E = 0$ to $E = V_2$. The left-hand side of Eq. (9) is plotted on the vertical axis in arbitrary units. The zeroes of the function, points where it touches the energy axis, are solutions to Eq. (9) and represent the energy eigenvalues for the system.

Figure 2 shows the transcendental function for a barrier of near zero width.[4] If we number the eigenvalues in order of increasing energy (beginning with $n = 1$ for the ground state), we observe an approximate n^2 dependence of the energy levels typical of the eigenvalues for the infinite square well without a barrier.

In Fig. 3, the barrier occupies 0.3% of the well's width. Here the tanh term in Eq. (9) becomes appreciable and lifts the entire function so that the roots occur in definite odd-even pairs. A comparison with Fig. 2 shows that although roots corresponding to even n have not changed substantially, those for odd n have moved upwards in energy.

This can be understood by considering the wave functions corresponding to neighboring odd and even eigenvalues: the $n = 1$, $n = 2$ pair will be described here as an illustration. For zero barrier width the wave functions are $n = 1$ – a half-period sine wave with an antinode in the center of the well; and $n = 2$ – a full-period sine wave with a node in the center. The changes in these functions, as a barrier of fixed height begins to grow in the center of the well, are readily seen. The curvature of the functions in the region occupied by the barrier will decrease, becoming negative for wave functions representing energies below the barrier height V_2. As the barrier widens, a dimple will be produced in the center of the symmetric ($n = 1$) wave function that will be forced towards zero amplitude there (see Fig. 6). In contrast, since the antisymmetric wave function ($n = 2$) is already small near the center of the well, curvature changes there produce only minor changes in the shape (Fig. 7). Thus the probability density function $\Psi^*\Psi$ for the symmetric wave function is almost identical to $\Psi^*\Psi$ for the antisymmetric wave function. The probability density functions are not quite identical since the symmetric wave function does not vanish at the center of the barrier. Reflecting these changes in the eigenfunctions, the $n = 1$ eigenvalue changes noticeably, increasing as the barrier width increases: the $n = 2$ eigenvalue moves upward more slowly, so that the difference between the two energies decreases. The drift of the $n = 2$ eigenvalue towards higher energies is characteristic of the limit of a barrier nearly filling the well, where the low-lying eigenvalues will approach those of an infinite well of width L_1 ($\ll L_3$).

The 0.5% barrier system in Fig. 4 shows more pronounced behavior of the sort already cited. Here, we note an interesting empirical fact: as the barrier widens, the energy difference between each odd root and its even partner approaches an unexpected regularity. The energy difference between the odd root n and the even root $n + 1$ is very nearly (four significant figures with a 0.5% barrier) equal to $(n/2 + 1/2)^2$ times the energy difference between the first odd root ($n = 1$) and the first even root ($n = 2$). In other terms,

$$E_{n+1} - E_n \cong [(n + 1)/2]^2(E_2 - E_1). \quad (10)$$

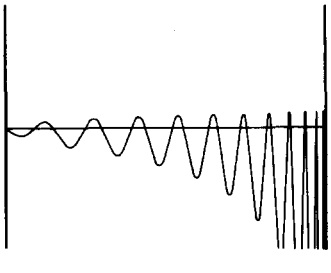

Fig. 3. Energy level function for a 0.3% barrier where the tanh rasies the entire function and slides the roots together.

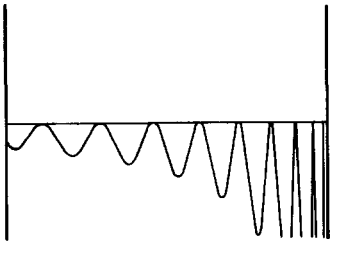

Fig. 5. Function for a 20% barrier has only 18 roots below the barrier height.

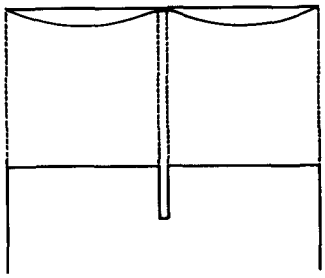

Fig. 6. Qualitative sketch of the symmetric wave function corresponding to the first energy eigenvalue.

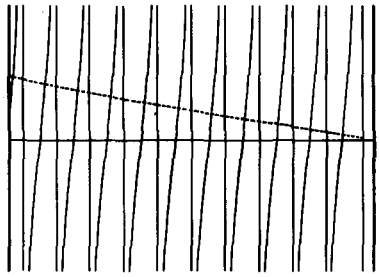

Fig. 8. Diagram of the simplified energy level function for odd roots.

This surprising fact greatly simplifies the search for eigenvalues, and finds an important application in Sec. IV's calculation of packet regeneration periods for a particle bound in a symmetric double well. Figure 5 represents a system in which the barrier occupies 20% of the well's width and demonstrates an aforementioned consequence of wider barriers. As the barrier widens, the transcendental stretches out along the energy axis. This causes the higher roots to slip above the height of the barrier. In this figure, the transcendental has only 18 roots below the barrier height, while the original function in Fig. 2 has 22 roots.[5]

As noted earlier, a quantitative search for the energy levels may be simplified by making use of the symmetry of the system. First, to ease later computations for the eigenfunctions, we redefine the constants of Eqs. (2)–(5) so that the size of the numbers involved stays within reason. Explicitly, we let $B' = B\exp(k_2L_3/2)$ and $C' = C\exp(-k_2L_3/2)$. The continuity equations at $x = L_1$ then become

$$\sin(k_1L_1) = B'/A\exp[k_2(L_1 - L_3/2)] + C'/A\exp[-k_2(L_1 - L_3/2)] \quad (11)$$

and

$$\cos(k_1L_1) = (k_2/k_1)\{B'/A\exp[k_2(L_1 - L_3/2)] - C'/A\exp[-k_2(L_1 - L_3/2)]\}. \quad (12)$$

Since wave functions corresponding to odd-(even-) numbered energy levels are symmetric (antisymmetric) about the center of the well, it is clear that $B' = C'$ ($B' = -C'$) for these wave functions. We discuss only the odd solutions here because the treatment for even solutions is quite similar. For odd solutions, the boundary conditions may be written as

$$\sin(k_1L_1) = 2B'/A\cosh k_2(L_1 - L_3/2) \quad (13)$$

and

$$\cos(k_1L_1) = 2B'/A(k_2/k_1)\sinh[k_2(L_1 - L_3/2)]. \quad (14)$$

Dividing the second equation by the first yields an equation whose roots are the odd-numbered energy eigenvalues:

$$\cot(k_1L_1) = (k_2/k_1)\tanh[k_2(L_1 - L_3/2)]. \quad (15)$$

The broken line in Fig. 8 is a graph of the right-hand side of this equation while the solid curves represent the left-hand side. The quantity plotted along the horizontal axis is (k_1L_1), which is proportional to $\sqrt{E}$. The vertical lines are values of (k_1L_1) equal to integral multiples of π, where the left-hand side of Eq. (15) is undefined.

Since the argument of the hyperbolic tangent function in Eq. (15) is always negative, the right-hand side must always be negative. Because of this, the two functions may intersect only where $\cot(k_1L_1)$ is negative. In other words, the qth odd root (i.e., root number $n = 2q - 1$) must occur in a region defined by $(q - 1/2)\,\pi < k_1L_1 < q\pi$. This fact leads to two useful results. First, since $k_1 = (2mE)^{1/2}/\hbar$, we can calculate upper and lower bounds for the qth odd energy level:

$$\frac{\hbar^2\pi^2(q - \frac{1}{2})^2}{2mL_1^2} < E_{2q-1} < \frac{\hbar^2\pi^2q^2}{2mL_1^2}. \quad (16)$$

Finally, since the same upper and lower bounds constrain the qth even energy level (root number $n = 2q$), we can calculate the total number of allowable energy eigenvalues below the barrier height by letting $E = V_2$ and solving the left inequality for q. The total number of roots below the barrier height is then found to be $2\,\mathrm{INT}\,[(2mV_2)^{1/2}L_1/\hbar\pi + \frac{1}{2}]$. (Here "INT" represents "integer part of.")

Having determined the number of roots with $E < V_2$, upper and lower bounds for each root, and the spacing relationship for adjacent pairs of roots [Eq. (10)], a simple bisection procedure will locate them. Eigenvalues of the system with $E > V_2$ closely approximate the eigenvalues of the infinite well with width L_3, and this allows good initial guesses in an iterative procedure involving Eq. (15).

This numerical determination of the eigenvalues enables straightforward evaluation of the coefficients B, C, (or B', C') and D. The constant A is set to satisfy the normalization condition. Equations (2)–(5) can thus be numerically evaluated to give the eigenfunctions. The wave packets, whose time dependence is the next subject of interest, are formed from linear combinations of these eigenfunctions.

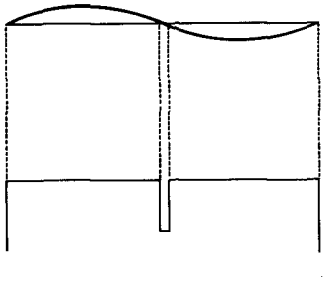

Fig. 7. Qualitative sketch of the antisymmetric wave function corresponding to the first even energy level.

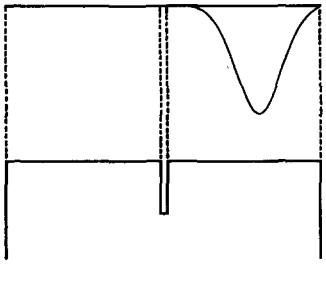

Fig. 9. Original wave packet at $t = 0$ with a diagram of the well.

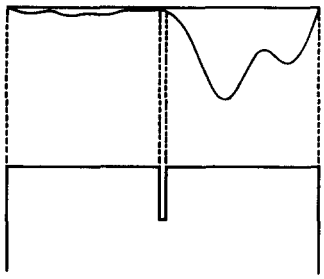

Fig. 10. Wave packet has melted and the right part sloshed against the barrier.

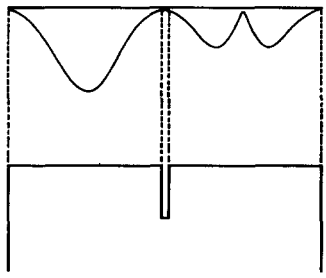

Fig. 12. Wave packet at one-half the predicted packet period.

IV. WAVE PACKET CONSTRUCTION AND TIME EVOLUTION

The solutions to Schrödinger's equation as described above form a complete, orthogonal set of functions of x, $0 < x < L_3$ at any time t. Because of this, arbitrary functions of x in this range may be written as a linear combination of these solutions. We chose to study a packet whose initial shape approximates a Gaussian:

$$f(x) = \exp\{-[(x - x_0)/\sigma]^2\} \cong \sum_m A_m \Psi_m(x,0); \qquad (17)$$

where each A_m is a time-independent coefficient. No set of A_m will make this relationship exact, since $f(x)$ does not vanish at the region boundaries $x = 0$, $x = L_3$. If, however, $\sigma \ll L_3$ and $x_0 \gg \sigma$, $(L_3 - x_0) \gg \sigma$, a very close approximation to $f(x)$ can be made by choosing the A_m to be the Fourier coefficients

$$A_m = \int_{x=0}^{x=L_3} \Psi_m^*(x,0) f(x) dx. \qquad (18)$$

It is easily demonstrated that, due to symmetry, the momentum expectation value for this packet is zero. Using such a packet, we can study its spreading without the additional complications of overall motion and scattering.[5] We present results for the wave packet whose initial probability distribution is shown in Fig. 9. The well barrier in this case is 2%, and the Gaussian width is $\sigma = 0.2L_3$. To follow the evolution of this packet in time, we simply evaluate the sum $\Sigma_m A_m \Psi_m(x,t)$ and plot the absolute value squared of the result, for various values of t.

In Fig. 10, the original wave packet, which was localized in the left side of the well, has dissolved into a right moving and a left moving part, and the right lobe has sloshed against the barrier. Through quantum tunneling, some of the strength has seeped into the right side of the well. In Fig. 11, the wave packet has sloshed back and forth several times and more strength has found its way into the right half of the well.

Figure 12, depicting a yet later stage of evolution, shows a situation in which more than half the probability density is present in the right-hand half of the well. At a time roughly twice that of Fig. 12, the wave packet has essentially reformed into its $t = 0$ shape (Fig. 13). The time elapsed between the situations depicted by Figs. 9 and 13 is referred to as the packet regeneration period.

The regeneration phenomenon has been demonstrated in other, similar, situations. Deutchman[6] has described it for a finite depth symmetric double well, using a simple wave packet made up of equal parts of the first and second eigenfunction. Segre and Sullivan,[2] in their study of an infinite square well with a delta function barrier, point out that wave packets in an infinite square well must regenerate since all excited-state energies are integer multiples of the ground-state energy. Since every eigenfunction in this case is periodic with a frequency E_n/h, all wave packets made up of such waves must reform with a period of h/E. The evolution of such a packet in a well without a barrier is illustrated in Figs. 14, 15, and 16.

Since the energy eigenvalues in a symmetric double well are not multiples of the first energy eigenvalue, the procedure outlined above does not produce the packet regeneration period for a wave packet bound in such a well. To solve this problem, we make an analogy to the well-studied phenomenon of beats formed by two waves of nearly equal frequency. The wave packet thus formed is characterized by a beat frequency equal to the frequency difference of the two component waves. In a similar fashion, we define a beat frequency, ν_b, for the first pair of wave functions in the double well: $\nu_b = (E_2 - E_1)/h$.

Because the energy difference between each pair of eigenvalues is small compared to the eigenvalues and is a multiple of the energy difference between the first pair of eigenvalues, we reason that the beat frequency already calculated is equal to the packet frequency in the symmetric double well. This gives

$$\tau = 1/\nu_b = h/(E_2 - E_1). \qquad (19)$$

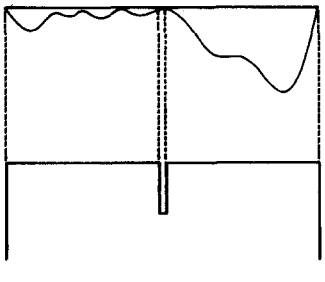

Fig. 11. Wave packet, pictured several collisions later.

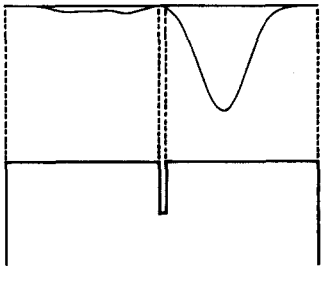

Fig. 13. Wave packet at a full period.

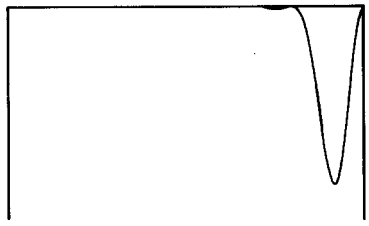

Fig. 14. Wave packet in an infinite square well pictured at one full period, essentially identical to its shape at $t = 0$.

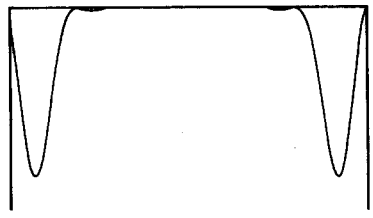

Fig. 16. Infinite square well wave packet at one-quarter period. Although each lobe is smaller than the original, they appear the same size because of scaling.

Figures 12 and 13, graphs of $\Psi^*\Psi$, at $t = \tau/2$ and $t = \tau$, respectively, confirm this prediction. Even though a small amount of probability remains on the right-hand side in Fig. 13 due to truncation and round-off errors in the computation the wave packet only approaches its original form when t is an integral multiple of τ. It is interesting to note that the regeneration period is a function of the well parameters, but not of those of the wave packet.

V. CONCLUSION

In the development of the above work, computer graphics played a crucial role. In the search for eigenvalues of the Schrödinger equation, computer generated plots such as those of Figs. 2–5 were suggestive of regularities for the eigenvalues that were not previously suspected. A search for a quantitative description of these regularities led to the result expressed in Eq. (10), and the streamlined procedure for finding energies described in Sec. III above. Observing the time behavior of wave packets within the well using computer generated graphs (as in Figs. 9–13) leads to an investigation of the phenomenon of regeneration, leading to an accurate, albeit approximate, analytic formula for the regeneration period [Eq. (19)].

The particular potential investigated in this paper is not without analogy in the physical world. The potential felt by the nitrogen atom in the NH_3 molecule can be approximated by such a symmetric double well. The existence of close lying energy level pairs, and the presence of a low, regeneration frequency (producing what is known as the inversion spectrum) is experimentally established.[7] Experimental data for heavy ion collisions at energies where "quasi-molecules" are expected to be formed by the two colliding nuclei, also show tendencies towards energy level pairs.[8] The double well should also provide a reasonable qualitative description in this case.

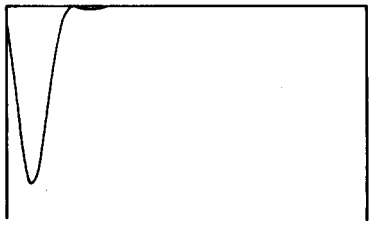

Fig. 15. Infinite square well wave packet at one half-period.

ACKNOWLEDGMENTS

The computations for this work were performed on the Washington and Lee University Harris/6 computer, and the plots were made on a Tektronix 4024 graphic display terminal. The authors are indebted to the Washington and Lee Computing Center Staff for their time and assistance.

[1] A. Goldberg, H. M. Schey, and J. L. Schwartz, Am. J. Phys. **35**, 177 (1967); **36**, 454 (1968).

[2] C. U. Segre and J. D. Sullivan, Am. J. Phys. **44**, 729 (1976).

[3] A. P. French and E. F. Taylor, *An Introduction to Quantum Physics* (Norton, New York, 1978).

[4] Solutions to Schrödinger's equation for the well shown in Fig. 1 depend only upon two parameters which can be chosen as follows: $(2mV_2L_3^2)^{1/2}/\hbar$, a unitless parameter which specifies the capacity of the well below the barrier top; and $(L_2 - L_1)/L_3$, which characterizes the fraction of the well filled by the barrier. For figures in this paper which depend upon specific values for these parameters, the first is set equal to 72, while the second is given in the text.

[5] Study of finite depth rectangular wells leads to the approximate proportionality between the number of bound states and $\sqrt{(VL^2)}$, where V is the well depth and L the well width (see, e.g., Ref. 3). It is thus not surprising to note that as the barrier reduces the area at the bottom of the well by 20%, the number of states below the barrier decreases by the same amount (22 to 18).

[6] P. A. Deutchman, Am. J. Phys. **39**, 952 (1971).

[7] See, for example, U. Fano and L. Fano, *Physics of Atoms and Molecues* (University of Chicago, Chicago, 1972), pp. 478–481.

[8] See P. Marmier and E. Sheldon, *Physics of Nuclei and Particles* (Academic, New York, 1970), Vol. II, pp. 1006–1013 and references therein.